

Photoneutron Cross Sections for V^{51} and Co^{59}

S. C. FULTZ, R. L. BRAMBLETT, J. T. CALDWELL, N. E. HANSEN, AND C. P. JUPITER

Lawrence Radiation Laboratory, University of California, Livermore, California

(Received July 12, 1962)

The (γ, n) and $(\gamma, 2n)$ cross sections for Co^{59} and V^{51} have been measured, using nearly monochromatic photons obtained from the annihilation in flight of fast positrons. The integrated cross sections up to 28 MeV for $\sigma(\gamma, n)$ and $\sigma(\gamma, 2n)$, respectively, are 0.447 ± 0.044 and 0.139 ± 0.014 MeV-b for Co, and 0.451 ± 0.045 and 0.106 ± 0.011 MeV-b for V. The minus-second cross sections (σ_{-2}) are 1.82 and 1.56 mb/MeV, respectively, for these elements. The level density parameters a were determined to be 5.49 and 6.18 MeV $^{-1}$, respectively. The quadrupole moments determined from the compound-nucleus formation cross sections, $\sigma(\gamma, n) + \sigma(\gamma, 2n) + \sigma(\gamma, np)$, were found to be 0.94 ± 0.13 and 0.66 ± 0.09 b, respectively, for Co and V.

INTRODUCTION

THE absorption of dipole radiation in the nucleus has been treated as a hydrodynamical problem by Steinwedel and Jensen.¹ The expression given for the shape of the cross-section curve for photon absorption is

$$\sigma = 8\pi \frac{NZ}{A} \frac{m}{M} \frac{\hbar c}{e^2} \frac{1}{(R^2/\lambda_0^2) - 2} \frac{2mc^2}{\hbar\gamma} \left(\frac{e^2}{2mc^2} \right)^2 \sin^2\phi. \quad (1)$$

Here N , Z , and A denote the neutron number, atomic number, and mass number, respectively, of the absorbing nucleus. M and m denote masses of the nucleus and nucleon, respectively, R is the radius of the nucleus, λ_0 is the wavelength of the lowest characteristic oscillation of the nuclear fluid, and γ is the viscosity constant of the fluid. ϕ is the phase angle between the external excitation field strength and the induced nuclear dipole moment. From dispersion theory,

$$\sin^2\phi = \frac{1}{1 + (\omega^2 - \omega_0^2)^2/\gamma^2\omega^2}, \quad (2)$$

where ω and ω_0 denote the angular frequencies of the external field at energy E and at the resonance energy E_0 , respectively. Equation (1) may be written in the simple form designated as a "Lorentz" line:

$$\sigma = \frac{\sigma_0}{1 + (E^2 - E_0^2)^2/\Gamma^2 E^2}, \quad (3)$$

where σ_0 denotes the peak cross section at energy E_0 , E is the energy of the external field, and $\Gamma = \hbar\gamma$ is the full width at half-maximum of the "resonance" curve. It may now be observed that all the terms which make up σ_0 are constant, and thus independent of the energy of the external radiation field.

The hydrodynamical treatment has been extended to deformed nuclei by Danos² and Okamoto.³ They

* Work performed under the auspices of the U. S. Atomic Energy Commission.

¹ H. Steinwedel and J. H. D. Jensen, *Z. Naturforsch.* **5a**, 413 (1950).

² M. Danos, *Nuclear Phys.* **5**, 23 (1958).

³ K. Okamoto, *Progr. Theoret. Phys. (Kyoto)* **15**, 75 (1956).

show that if a nucleus is spheroidal in shape, it will exhibit two characteristic resonances, ω_b and ω_a . The cross-section curve or nuclear excitation function will, therefore, contain two resonance components or Lorentz lines with the characteristics described by

$$\omega_b/\omega_a = 0.911(\alpha/\beta) + 0.089, \quad (4)$$

where ω_b and ω_a denote the resonance frequencies (energies) of the two Lorentz components; α and β denote the lengths of the semimajor and semiminor axes of the spheroid. If the nucleus has a positive quadrupole moment, a necessary consequence of the theory is that

$$2\sigma_a\Gamma_a = \sigma_b\Gamma_b, \quad (5)$$

where σ_a and Γ_a denote, respectively, the peak cross section and width of the low-energy resonance line, while σ_b and Γ_b are the peak cross section and width of the high-energy resonance component. Integration of Eq. (3) gives

$$\left(\int_0^E \sigma(E) dE \right) / \sigma_0 \Gamma = \frac{1}{2} \tan^{-1} \left(\frac{KX}{1-X^2} \right) - \frac{K}{8(1-K^2/4)^{1/2}} \times \ln \left(\frac{\{X + [1 - (K/2)^2]^{1/2}\}^2 + (K/2)^2}{\{X - [1 - (K/2)^2]^{1/2}\}^2 + (K/2)^2} \right), \quad (6)$$

where $K = \Gamma/E_{\max}$ and $X = E/E_{\max}$. Also,

$$\int_0^\infty \sigma(E) dE = \frac{\pi}{2} \sigma_0 \Gamma. \quad (7)$$

A comparison with the Breit-Wigner equation is of interest. This is given by

$$\sigma = 4\pi\lambda^2 \frac{\Gamma_n\Gamma_\gamma}{4(E-E_R)^2 + \Gamma^2},$$

where E_R denotes the resonance energy. Γ_n and Γ_γ are the (respective) probabilities for decay of the compound nucleus by emission of a neutron or a gamma ray, and $\Gamma = \Gamma_n + \Gamma_\gamma$. Then

$$\sigma = \frac{\sigma_0}{[2(E-E_R)/\Gamma]^2 + 1}, \quad (8)$$

where $\sigma_0 = 4\pi\lambda^2\Gamma_n\Gamma_\gamma/\Gamma^2$. It can be seen that σ_0 contains the wavelength term, λ^2 , which is dependent upon the energy of the incident photon. A Breit-Wigner fit to the resonance line is, therefore, not easily applicable to analysis of structure in the photoneutron giant resonance.

A number of measurements have been previously undertaken at other laboratories in an effort to establish the presence of structure in the giant dipole resonance. In all cases, the data have been obtained by the use of continuous bremsstrahlung radiation, and, therefore, contain features characteristic of the method. For such a method, the cross section is obtained by unfolding the bremsstrahlung spectra from integral-type activation or neutron-yield curves. The yield curves usually exhibit a high slope just above the (γ, n) threshold, which gradually diminishes as the curve flattens out at high energies. The analysis in the region above the peak of the giant resonance therefore involves obtaining small differences between large numbers, a process which leads to large errors in a region where the shape of the giant resonance needs to be well established. An additional factor which has contributed to uncertainty in the shape of the giant resonance in former works has been the estimation of the contributions to the cross sections from the higher multiplicity, $(\gamma, 2n)$ and $(\gamma, 3n)$, reactions. Few measurements have been made, and in general the higher multiplicities have been calculated. The determinations of the level density parameters used in such calculations were usually based upon rough assumptions, or approximated by comparison with some measurements. As a consequence the contributions from the higher multiplicity reactions remained largely undetermined, leading to considerable uncertainty in the shape of the giant resonance. A third factor, which has also affected the quadrupole moment calculations as based upon analysis of bremsstrahlung data, has been the manner in which Lorentz curves have been fitted. In most cases, values for the six parameters open to choice were somewhat arbitrarily chosen until two sets were found which reasonably fitted the experimental curve, along with the condition expressed in Eq. (5). However, the contributions to the integrated cross section from energy regions beyond the upper energy limit of the measurements were not accounted for.

The measurements and analysis undertaken for the present report attempt to overcome the areas of uncertainty discussed above. The measurements were made with the use of essentially monochromatic gamma rays, so that no unfolding procedure of the nature described above was necessary. The higher multiplicity contributions to the cross sections were directly measured, and consequently the level density parameters were also measured. A system for analysis of the giant resonance for formation of the compound nucleus was developed, whereby contributions to the cross sections beyond the energy range of the measure-

ments are taken into account, and the measured integrated cross sections are utilized. In this manner arbitrariness in the choice of the values for the six parameters is much reduced.

APPARATUS AND PROCEDURE

The measurements of the photoneutron cross sections for V⁵¹ and Co⁵⁹ described herein were obtained by use of a newly developed technique⁴⁻⁷ using monochromatic photons obtained from the annihilation in flight of fast positrons. The positrons were created by pair production from 10-MeV bremsstrahlung, at the center of a two-section linear electron accelerator, and were accelerated in the second section to the desired energy. They were then magnetically analyzed and made to pass through a thin target of Be or LiH. The photons created arise from the two-photon annihilation of the positrons with electrons in the target material. In the forward direction they have energies 0.76 MeV greater than the energies of the positrons, for the range of positron energies used in the present experiment. The resolution of the photons was approximately 3%.⁸

The photons were measured by use of a transmission ion chamber filled with xenon to a pressure of 1 atm. The ion chamber was calibrated by use of a NaI(Tl) gamma-ray spectrometer having a cylindrical crystal 6 in. long \times 5-in. diam. The neutrons emitted by the sample were detected in a 4π paraffin-moderated neutron detector, having a 3-in.-diam axial hole along the direction of the photon beam. The detector contained 24 BF₃ proportional counters, each filled with BF₃ to 120-cm pressure.

The photoneutron sample consisted of 6 or 7 disks of metal, each 2 in. in diameter and 0.25 in. thick. The metal disks were rigidly mounted in a container constructed of plastic foam and were spaced equally over a length of 4 in. The sample container was placed at the center of the neutron detector. Measurements were made simultaneously on the neutron yield and the number of gamma rays for a number of chosen positron energies ranging from 8.5 to 28 MeV. The magnetic fields of all magnets were then reversed and the negative halves of the pairs were selected in order to obtain a beam of negative electrons of similar intensity to that of the positrons. For each selected energy of negative electrons, simultaneous measurements were made on the neutrons and photons until a range of

⁴ C. P. Jupiter, N. E. Hansen, R. E. Shafer, and S. C. Fultz, *Phys. Rev.* **121**, 866 (1961).

⁵ J. Miller, C. Schuhl, G. Tamas, and C. Tzara, *J. Phys. Radium* **21**, 296 (1960).

⁶ F. D. Seward, S. C. Fultz, C. P. Jupiter, and R. E. Shafer, University of California Radiation Laboratory Report UCRL-6177, 1960 (unpublished).

⁷ S. C. Fultz, R. L. Bramblett, J. T. Caldwell, and N. A. Kerr, University of California Radiation Laboratory Report UCRL-6681 (1962); *Phys. Rev.* **127**, 1273 (1962).

⁸ C. R. Hatcher, R. L. Bramblett, N. E. Hansen, and S. C. Fultz, *Nuclear Instr. and Methods* **14**, 337 (1961).

energies corresponding to those examined with the positrons had been covered. From the positron and negative electron data obtained in this manner, the contributions of the positron bremsstrahlung to the neutron counting data, could be deduced, and subtracted from the neutron data.

The gating interval for the neutron counters was 335 μ sec. The neutron counts were separated electronically as single, double, or triple counts during the gating interval (i.e., per beam pulse). Statistical analysis was applied to the data, and the neutron counts recorded per beam pulse were correlated to the number of neutrons emitted per nuclear disintegration. The cross sections for the (γ, n) and $(\gamma, 2n)$ reactions were then deduced. More details of the experimental procedure are given in a previous report.⁷

EXPERIMENTAL RESULTS

A. $Co^{59}(\gamma, n)$ and $(\gamma, 2n)$ Cross Sections

The total photoneutron cross section for Co has been measured at other laboratories. Montalbetti and Katz⁹ give a peak cross section of 130 mb at 16.9 MeV and a width of 5.4 MeV. The integrated cross section given was 0.750 MeV-b, for $\sigma(\gamma, n) + 2\sigma(\gamma, 2n) + \sigma(\gamma, np)$. Fluornoy, Tickle, and Whitehead¹⁰ show a peak cross section of approximately 110 mb at about 16.75 MeV, and a second peak near 19 MeV with a width of approximately 6 MeV. The cross section curve, corrected for multiplicity, was resolved into two Breit-Wigner components a and b having the parameters E_a , Γ_a , and σ_a of 16.5 MeV, 2.0 MeV, and 78 mb, respectively, and E_b , Γ_b , and σ_b with values of 19.0 MeV, 4.0 MeV, and 78 mb. The integrated cross section up to 25 MeV was found to be 0.709 MeV-b. In addition, the energy spectrum of photoneutrons emitted from cobalt has been measured by the photographic-track method and compared with that which would be expected from the evaporative model.¹¹ Hartley, Stephens, and Winhold¹² have measured the photoneutron cross section of Co using $Li^7(p, \gamma)$ gamma rays. They give 23 and 47 mb for the cross sections at 14.4 and 17.6 MeV, respectively.

The results of the measurements on Co described in the present report are shown in Figs. 1-3. In Fig. 1 is shown the initial neutron data reduced to cross sections. The upper curve or total neutron yield curve consists of the cross sections $\sigma(\gamma, n) + 2\sigma(\gamma, 2n) + \sigma(\gamma, np)$. Contributions from $\sigma(\gamma, p)$ were not measured, but work of Toms and Stephens¹³ indicates that the yield of protons to neutrons is about 0.20, for photon energies

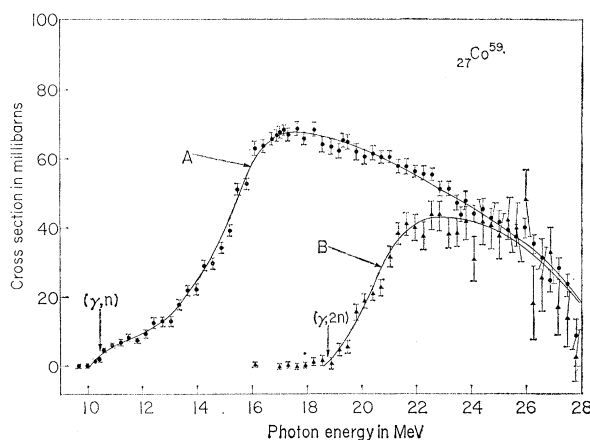


FIG. 1. Cross sections for Co from neutron yield data. Curve A consists of $\sigma(\gamma, n) + 2\sigma(\gamma, 2n) + \sigma(\gamma, np) + 3\sigma(\gamma, 3n)$ and was obtained from single-neutron counting data. Curve B consists of $2\sigma(\gamma, 2n) + 6\sigma(\gamma, 3n)$ and was obtained from double-neutron counting data.

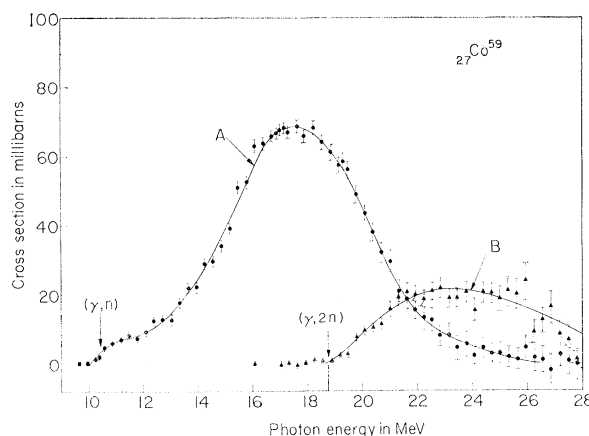


FIG. 2. Partial cross-section curves for Co. Curve A consists of $\sigma(\gamma, n) + \sigma(\gamma, np)$. Curve B consists of $\sigma(\gamma, 2n) + 3\sigma(\gamma, 3n)$.

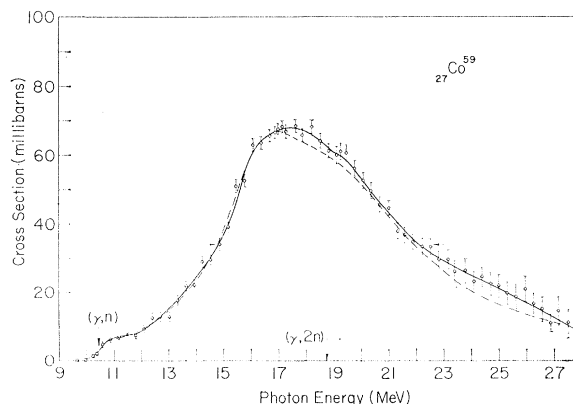


FIG. 3. The formation cross section, $\sigma(\gamma, n) + \sigma(\gamma, 2n) + \sigma(\gamma, np)$ for the compound nucleus Co^{59} . The solid curve represents an average line through the data points. The dashed curve is the sum of two Lorentz lines with parameters given in Table I.

⁹ R. M. Montalbetti, L. Katz, and J. Goldemberg, Phys. Rev. **91**, 659 (1953).

¹⁰ P. A. Fluornoy, R. S. Tickle, and W. D. Whitehead, Phys. Rev. **120**, 1424 (1960).

¹¹ V. Emma, C. Milone, and A. Rubbino, Nuovo cimento **22**, 135 (1961).

¹² W. H. Hartley, W. E. Stephens, and E. J. Winhold, Phys. Rev. **104**, 178 (1956).

¹³ M. E. Toms and W. E. Stephens, Phys. Rev. **95**, 1209 (1954).

up to 24 MeV. Contributions from $\sigma(\gamma,3n)$ would be negligible since the calculated $(\gamma,3n)$ threshold is 30.4 MeV.

It is evident from Fig. 1 that the peak cross section of the total neutron yield curve is approximately 68 mb at 17.5 MeV. The width at half-maximum, Γ , for this curve is about 11.5 MeV. This is considerably broader than any previously reported for Co. The $\sigma(\gamma,n)$ and $\sigma(\gamma,2n)$ curves are shown in Fig. 2. The $\sigma(\gamma,n)$ curve was obtained by subtracting the lower curve from the upper curve in Fig. 1. The $\sigma(\gamma,2n)$ curve was obtained from analysis of the double-neutron-counting data. The $\sigma(\gamma,n)$ curve has a peak value of 68 mb at 17.5 MeV, and a Γ value of 5.9 MeV. The $\sigma(\gamma,2n)$ curve has a peak of 20.2 mb at about 23.5 MeV. The integrated cross sections for $\sigma(\gamma,n)$ and $\sigma(\gamma,2n)$ up to 28 MeV are 0.447 ± 0.044 and 0.139 ± 0.014 MeV-b, respectively. The cross section data shown in Fig. 3 consist of the sum of data from the two curves of Fig. 2, and constitutes the formation cross section. The integrated value for the formation cross section is 0.586 ± 0.058 MeV-b. The addition of another 20% to account for the contribution from $\sigma(\gamma,p)$ would raise the integrated cross section to 0.70 MeV-b.

B. $V^{51}(\gamma,n)$ and $(\gamma,2n)$ Cross Sections

The photoneutron cross section of vanadium has been measured by use of bremsstrahlung radiation. Nathans and Halpern¹⁴ report a peak cross section of 98 mb at 18.7 MeV, a width of 5.8 MeV and an integrated cross section of 0.625 MeV-b. Goldemberg and Katz¹⁵ found a peak cross section of 100 mb at 17.7 MeV, a width of 5.4 MeV and an integrated cross section of 0.59 MeV-b.

Results from the present measurements on vanadium are shown in Fig. 4. The excitation function for the

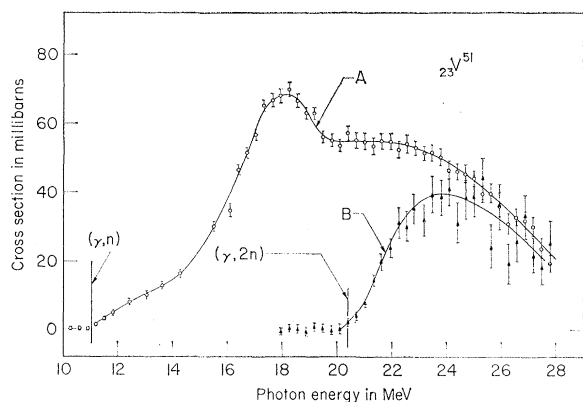


FIG. 4. Cross sections for V from neutron yield data. Curve A consists of $\sigma(\gamma,n) + 2\sigma(\gamma,2n) + \sigma(\gamma,np) + 3\sigma(\gamma,3n)$ and was obtained from single-neutron counting data. Curve B consists of $2\sigma(\gamma,2n) + 6\sigma(\gamma,3n)$ and was obtained from double-neutron counting data.

¹⁴ R. Nathans and J. Halpern, Phys. Rev. **93**, 437 (1954).

¹⁵ J. Goldemberg and L. Katz, Can. J. Phys. **32**, 49 (1954).

total neutron yield (top curve) has a peak of 68.4 mb at 18.25 MeV, and a broad second peak at a higher-energy. The width of the total photoneutron cross-section curve is approximately 10 MeV, which is considerably broader than the values previously reported. The lower curve was obtained from the double neutron counts, and represents $2\sigma(\gamma,2n)$. Contributions from $(\gamma,3n)$ reactions are negligible since the $(\gamma,3n)$ threshold is 31.9 MeV. A rough estimate of the amount of (γ,p) reaction can be obtained from the F curves given by Blatt and Weisskopf.¹⁶ These indicate that about 22% of the total interactions with gamma rays can be attributed to (γ,p) reactions. The measured $(\gamma,2n)$ threshold is 20.25 ± 0.3 MeV, which compares favorably with the value 20.38 given from mass data.¹⁷ The (γ,n) and $(\gamma,2n)$ cross section curves are shown in Fig. 5. For the $\sigma(\gamma,n)$ curve, a peak cross section of 68 mb occurs at 18.25 MeV, with a width of 6.0 MeV. The $\sigma(\gamma,2n)$ curve has a peak of about 20 mb at 23.75 MeV. The integrated cross sections up to 28 MeV for the $\sigma(\gamma,n)$ and $\sigma(\gamma,2n)$ curves are 0.451 ± 0.045 and 0.106 ± 0.011 MeV-b. The formation cross section for the compound nucleus is obtained from the sum of the data from the $\sigma(\gamma,n)$ and $\sigma(\gamma,2n)$ curves, and is given in Fig. 6. The integrated cross section is 0.557 ± 0.056 MeV-b. The (γ,p) reactions would contribute roughly 22% to the integrated cross section, increasing it to 0.68 MeV-b.

ANALYSIS OF THE DATA

In order to fit two Lorentz lines to a giant resonance cross-section curve, six parameters (σ_a , Γ_a , E_a , σ_b , Γ_b , and E_b) are open to choice. This could lead to considerable arbitrariness in choice, and hence the lack of a unique determination for E_b/E_a . A special procedure was therefore set up for fitting the nuclear

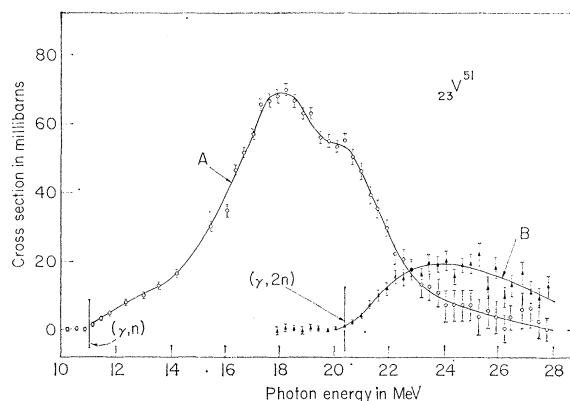


FIG. 5. Partial cross-section curves for V. Curve A consists of $\sigma(\gamma,n) + \sigma(\gamma,np)$. Curve B consists of $\sigma(\gamma,2n) + 3\sigma(\gamma,3n)$.

¹⁶ J. M. Blatt and V. F. Weisskopf, *Theoretical Nuclear Physics* (John Wiley & Sons, Inc., New York, 1952), Chap. 8.

¹⁷ L. A. Koenig and J. E. Mattauch, *Nuclear Data Tables* (Published by U. S. Atomic Energy Commission, 1960).

formation cross sections for Co and V with Lorentz lines. It was designed to reduce the arbitrariness in choice of the above parameters. For this procedure the integrated cross section over the energy range of the measurements must be known, and Eq. (5) is assumed to be valid. On inspection of the cross-section curve, one may make an estimate of E_b , where the peak cross section for the b or high-energy component Lorentz line should lie. A value for Γ_b (for example, about 7 MeV) is then chosen. From these choices, and the use of Eqs. (6) and (7), it is possible to set down the conditions relating the integrated cross section to the areas under the component Lorentz lines:

$$(\pi/2)\sigma_a\Gamma_a - W_a + (\pi/2)\sigma_b\Gamma_b - W_b = A, \quad (9)$$

where $A = \int_{E_n}^{28} \sigma(E) dE$, is the integrated cross section between threshold and the upper energy limit of the measurements. W_a and W_b are the "wing corrections" for the Lorentz lines, and include the areas under the curves a and b between zero and the threshold energy, added to that between the upper limit and infinite energy. σ_a and σ_b denote the peak values of the Lorentz lines. W_a and W_b can be deduced from Eq. (6). Thus, from Eq. (5) we get

$$(\pi/2)(\sigma_b\Gamma_b/2 + \sigma_b\Gamma_b) - (W_a + W_b) = A. \quad (10)$$

To evaluate W_a , a good initial assumption is $\Gamma_a = \frac{1}{2}\Gamma_b$, and E_a may be taken (by inspection) as approximately 3 MeV below E_b . The wing correction term of Eq. (10) is insensitive to the choice of E_a , especially so since W_a is only about half the value of W_b . Thus, E_b and Γ_b have been chosen, and σ_b can be determined from Eq. (10). The Lorentz line having the parameters E_b , Γ_b , and σ_b designated as curve "b" can now be determined, and subtracted from the experimental curve $\sigma(\gamma, n) + \sigma(\gamma, 2n)$. The remainder curve represents a tentative plot of the low-energy Lorentz curve. If the choice of parameters E_b and Γ_b is correct it will be immediately apparent, since the remainder curve will be related to curve "b" by Eq. (5). If $2\sigma_a\Gamma_a$ is less than $\sigma_b\Gamma_b$, E_b has been chosen at too low an energy. If Γ_b has been chosen incorrectly, the slope of the sum of the analytic curves with parameters E_b , Γ_b , σ_b , and E_a , Γ_a , and σ_a disagrees with that of the experimental curve on the high energy side. By a few iterations it is thus possible to find two component Lorentz lines which satisfy Eqs. (5) and (10) and the shape of the experimental curve. It is usually found that there is very little range in the choice of values of E_b and Γ_b , for which these conditions can be satisfied. A unique

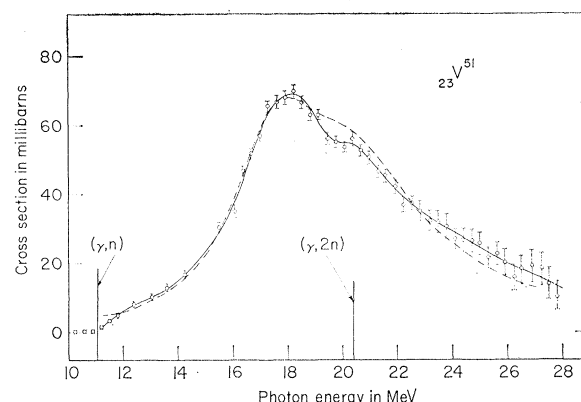


FIG. 6. The formation cross section $\sigma(\gamma, n) + \sigma(\gamma, 2n) + \sigma(\gamma, np)$ for the compound nucleus V^{51} . The solid curve represents an average line through the data points. The dashed curve is the sum of two Lorentz lines with parameters given in Table I.

determination of the values of E_a and E_b (or ω_a and ω_b) is therefore possible, and from this the intrinsic quadrupole moment, Q_0 , the eccentricity parameter, " ϵ ", and the lengths of the axes can be determined for a spheroidal nucleus.

The parameters deduced for the Lorentz line components for the $\sigma(\gamma, n) + \sigma(\gamma, 2n)$ curves of V and Co are given in Table I. The quadrupole moment and nuclear shape parameters are also given. The latter include semimajor axis α , semiminor axis β , and eccentricity parameter ϵ , where

$$\epsilon = (\alpha^2 - \beta^2)/R^2.$$

The sum of the Lorentz lines having the parameters given in Table I, are shown by the dashed lines in Figs. 3 and 6 for Co and V, respectively.

From the $\sigma(\gamma, 2n)$ and the nuclear formation cross-section curves, the ratio of $\sigma(\gamma, 2n)$ to the total cross section can be derived as a function of energy. An analytic expression for this ratio has been derived by Weisskopf¹⁶ based on a Fermi gas behavior of the nucleons:

$$\sigma(\gamma, 2n)/\sigma_{\text{tot}} = 1 - (1 + \epsilon_c/\theta) \exp(-\epsilon_c/\theta), \quad (11)$$

where $\theta = [(E - E_n)/a]^{1/2}$ and $\epsilon_c = E - E_{2n}$. E_n and E_{2n} are the thresholds for the (γ, n) and $(\gamma, 2n)$ reactions, and a is the level density parameter in units of MeV⁻¹. Equation (11) was applied to the experimental data for Co and V. The level density parameters, a , so obtained are given in Table II.

TABLE I. Lorentz line and nuclear shape parameters for Co and V.

Element	σ_a (mb)	Γ_a (MeV)	E_a (MeV)	σ_b (mb)	Γ_b (MeV)	E_b (MeV)	Q_0 (b)	α (10^{-13} cm)	β (10^{-13} cm)	ϵ
Co ⁵⁹	40	3.75	16.5	43.4	7.0	19.25	0.94	5.53	4.68	0.355
V ⁵¹	41	3.60	17.5	46	6.5	20.25	0.66	4.40	5.15	0.336

TABLE II. Integrated cross sections and nuclear level density parameters. σ_{tot} includes estimated contributions for (γ, p) reactions.

Element	σ_{-2} (mb/MeV)	$0.00225A^{5/3}$ (mb/MeV)	a (MeV $^{-1}$)	$\int_0^{28} \sigma dE$ (MeV-b)	$\int_0^{28} \sigma_{\text{tot}} dE + W$ (MeV-b)	$0.06 NZ/A$ (MeV-b)
Co ⁵⁹	1.82	2.014	5.49	0.586	0.87	0.879
V ⁵¹	1.56	1.564	6.18	0.557	0.84	0.758

Also given in Table II are values of the integrated cross sections and of the second-moment cross sections,¹⁸ σ_{-2} , where $\sigma_{-2} = \int_0^{28} \sigma(E) E^{-2} dE$. Theoretical values of σ_{-2} are given in the third column. The experimentally determined integrated cross sections are given in the fifth column. In the sixth column are given the sums of the experimental integrated cross sections and the wing corrections. The theoretically derived integrated cross sections using the Thomas-Reiche-Kuhn sum rule are given in the seventh column. Estimated errors in the cross-section measurements, and quantities derived from them are approximately $\pm 10\%$, while those in the level density parameters are about $\pm 10\%$. Errors in the quadrupole moments are estimated $\pm 14\%$.

DISCUSSION AND CONCLUSIONS

It has been pointed out by Spicer¹⁹ that splitting of the giant resonances should be exhibited for nuclei with atomic numbers between 9 and 30, since there is evidence that a considerable number of nuclei in this range are highly deformed. Both V and Co giant resonances exhibit such splitting to a marked degree, and thus yield intrinsic quadrupole moments. It is of interest to compare the values of Q_0 so obtained with those obtained by other methods.

From Coulomb excitation data,²⁰ a 320-keV level with spin 5/2 is excited in V⁵¹. For this, the transition probability $B(E2)$ is 0.0056. The ground state of V⁵¹ has a spin 7/2 and the 320-keV level represents the lowest excited state. The intrinsic quadrupole moment, Q_0 , can be calculated for transitions of the type $I+1 \rightarrow I$, using the relation

$$B(E2) = \frac{15}{16\pi} Q_0^2 \frac{K^2(I+1-K)(I+1+K)}{I(I+1)(2I+3)(I+2)}.$$

Taking $K=3/2$ the value obtained for Q_0 is 0.636 b. Using 1.25 ($\pm 2\%$) fermis for the nuclear radius parameter of vanadium,²¹ data from the present experiment (Table I) gives 0.66 ± 0.09 b. Q_0 may also be calculated from the nuclear quadrupole moment measured by microwave spectroscopy. For V, the value of

Q_0 so obtained is 0.85 ± 0.3 b.²² From the present measurements on Co the value obtained for Q_0 is 0.94 ± 0.13 b on using the nuclear radius parameter of 1.27 ($\pm 2\%$) F.²¹ This may be compared with 0.90 ± 0.30 b which was deduced from spectroscopic data.²²

The integrated cross sections listed in the fifth column of Table II appear to be about 30% too low, when compared with the theoretical values (seventh column). It should be noted that the theoretically derived quantities have no contributions from the exchange force and are based upon an integration from zero to infinite energy. The addition of a correction for the (γ, p) reactions to the integrated cross section is only approximate since few measurements have been made. Toms and Stephens¹³ obtained 0.20 for Co which agreed with evaporative model calculations. However, Lin'Kova *et al.*²³ have found for Cu⁶⁵, which has a similar atomic number, that the contribution from the (γ, p) reactions is only 15%. Of this, 80% of the protons arise from direct interaction and only 20% from evaporation. An additional correction to the integrated cross sections arises from the fact that the measurements do not extend to infinite energy. If the Lorentz lines accurately describe the photon absorption process, then such corrections can be obtained by adding the area under the "wings" of the Lorentz lines, i.e., the areas between the upper energy limit of the measurements and infinite energy when the (γ, p) cross sections have been included. The results given in the sixth column of Table II include such wing corrections and corrections for the (γ, p) reactions as based upon evaporative model calculations. Thus, a more realistic comparison of the experimental values of the integrated cross section with theory is obtained by comparing the sixth and seventh columns of Table II. Better agreement is obtained in this case.

Values for σ_{-2} listed in Table II were computed from the nuclear formation cross sections (Figs. 3 and 6), and agree with those derived theoretically. When a correction for $\sigma(\gamma, p)$ is added in the manner described above, σ_{-2} attains the values 2.22 and 1.91 MeV $^{-1}$ for Co and V, respectively, which are approximately 11 and 22% greater than the theoretical values. For Co, the (γ, p) contributions have been measured, and the agreement of σ_{-2} values is within the estimated experimental errors. However, no data from (γ, p)

¹⁸ J. S. Levinger, *Nuclear Photodisintegration* (Oxford University Press, London, 1960).

¹⁹ B. M. Spicer, *Australian J. Phys.* **11**, 490 (1958).

²⁰ K. Alder, A. Bohr, T. Huus, B. Mottelson, and A. Winther, *Revs. Modern Phys.* **28**, 432 (1956).

²¹ R. Hofstadter, *Revs. Modern Phys.* **28**, 214 (1956).

²² R. J. Blin-Stoyle, *Revs. Modern Phys.* **28**, 75 (1956).

²³ N. V. Lin'Kova, R. M. Osokina, B. S. Ratner, R. Sh. Amirov, and V. V. Akindinov, *Soviet Phys.—JETP* **11**, 566 (1960).

measurements on V are available, so the correction is only a rough estimate based upon evaporative model calculations. The 22% discrepancy cannot therefore be regarded as highly significant.

The level density parameters a which have been listed in Table II were deduced by use of Eq. (11). In applying this expression, it was necessary to use values of E_{2n} which differ slightly from the $(\gamma, 2n)$ thresholds deduced from mass data. The values of E_{2n} used were computed on the assumption that the level density parameter is constant over an excitation energy range of 1 to 2 MeV, just above the $(\gamma, 2n)$ threshold, and were 20.54 and 19.22 MeV for V and Co, respectively. The corresponding $(\gamma, 2n)$ thresholds are 20.38 and 18.77 MeV, respectively.¹⁷ It is considered that the values used fall within the range expected from the use of several different mass tables. The values of the level density parameters for Co and V may be compared with those obtained from (n, n') experiments. For an excitation energy of 7 MeV, values of 9.4, 10.5,²⁴ and 6.4²⁵ MeV⁻¹ have been reported for vanadium. These may be compared with the value 6.18 ± 0.60 MeV⁻¹ obtained in the present experiment. For cobalt, using an excitation energy of 14 MeV, the value 7.8 MeV⁻¹ has been reported.²⁴ This may be compared with 5.49 ± 0.55 MeV⁻¹ obtained from the photoneutron multiplicity measurements.

It is apparent that the measurements reported above give nuclear parameters which are in reasonable agreement with theoretically determined values, and with those determined by other experimental methods. The experimental integrated cross sections should be corrected for the high-energy tails which occur above the

giant resonance, and for (γ, p) contributions. When this is done, the values agree well with those obtained through exhaustion of the Thomas-Reiche-Kuhn dipole sum rule. The quadrupole moments agree well with those deduced from microwave and Coulomb excitation measurements. They were deduced by taking into account the wing corrections to the Lorentz curves, using the experimental values of the integrated cross sections, and the theoretically derived fact that for a spheroidal nucleus $\Gamma_b \sigma_b = 2\Gamma_a \sigma_a$. The addition of the estimated $\sigma(\gamma, p)$ corrections to the nuclear formation cross sections did not alter the values obtained for the quadrupole moments. The values obtained for the level density parameters " a " agree reasonably well with those obtained from other laboratories. The measured σ_{-2} values are in reasonable agreement with those deduced on the basis of a simplified theoretical treatment. The magnitude of the Co cross section at 14.4 and 17.6 MeV agrees with the values obtained by use of the $Li(p, \gamma)$ gamma rays,¹² within the quoted experimental errors. It would therefore appear that the photoneutron measurements made with the use of nearly monochromatic gamma rays, and taking into account the neutron multiplicity of the photonuclear processes, yield values for nuclear parameters which agree with those deduced from relatively simplified theoretical treatments.

ACKNOWLEDGMENTS

The authors wish to express their thanks to G. A. Auchampaugh and Miss C. S. Lacey for assistance with analysis; to Dr. C. D. Bowman for help with some of the measurements and to Accelerator operating personnel for their cooperation. They also wish to acknowledge helpful suggestions from Dr. W. C. Barber of Stanford University.

²⁴ E. Erba, U. Facchini, and E. Saetta Menichella, *Nuovo cimento* 22, 1237 (1961).

²⁵ D. B. Thompson, Doctoral thesis, University of Kansas, 1960 (unpublished).